A Compact Double-Gate MOSFET Model Comprising Quantum-Mechanical and Non-Static Effects

G. Baccarani and S. Reggiani

DEIS, Università di Bologna
viale Risorgimento 2, 40136 Bologna, Italy

Abstract

A compact model for the Double-Gate MOSFET (DG-MOSFET) which fully accounts for quantum mechanical effects, including motion quantization normal to the Si-SiO_2 interface, band splitting into subbands and non-static effects in the transport model is worked out. The model holds both in subthreshold and strong inversion, and ensures a smooth transition between the two regions. A simplified energy-balance transport model is worked out which allows us to compare the drain-current calculations with Monte Carlo data.

1. Introduction

The Double-Gate MOSFET (DG-MOSFET) appears to be one of the most promising new device architectures for miniaturization below 0.1 μm [1]-[3], because the drain-induced barrier lowering is minimized by the shielding effect of the double gate. A previous Monte Carlo simulation of such a device [1] provided convincing evidence that the channel length can be reduced down to 30 nm for a silicon-film depth of 5 nm and an oxide thickness of 3 nm, with an acceptable short-channel effect. The predicted device transconductance turned out to be as large as 2.3 mS/μm and 1.3 mS/μm for n- and p-channel DG-MOSFETs.

2. Physical model

The model of the DG-MOSFET is depicted in figure 1. The quantization of the energy is associated with the motion along z. This results in two energy "ladders" of subbands (for a $\langle 100 \rangle$ surface crystal orientation), with two-dimensional densities of states: the charge density per unit of area of the quantized particles can be analytically calculated as follows

$$Q_c = -q \sum_{n=1}^{N_t} \sum_{k=1}^{N_m} N_k \log\{1 + \exp\left[-(E_{n,k} - E_{Fn})/k_B T\right]\}, \tag{1}$$

where $N_k = (m^*_{dk} k_B T)/(\pi \hbar^2)$ represents the density of states in the subband at energy $E_{n,k}$; m^*_{dk} is the density-of-states effective mass, N_t is the number of subbands generated by each minimum of the silicon conduction band, $N_m = 6$ is the number of

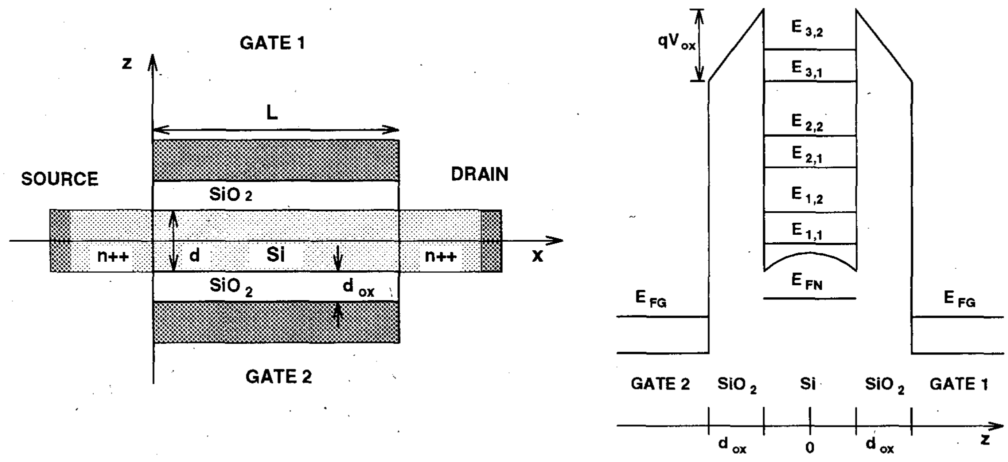

a b

Figure 1: Model of the DG-MOSFET. a) Cross-section: in this work, we consider $d = 5\,\mathrm{nm}$, $d_{ox} = 3\,\mathrm{nm}$ and the source-drain impurity concentration $N_D = 10^{20}\,\mathrm{cm}^{-3}$. b) Band diagram: E_{FG} and E_{Fn} represent the Fermi levels in the gate and the silicon channel, respectively.

minima, and E_{Fn} is the electron quasi Fermi level within the channel region. More specifically, for a silicon crystal with $\langle 100\rangle$ orientation, two energy eigenvalues with degeneracy factor $g_1 = 2$ and $g_2 = 4$ are created by the six minima in the conduction band. The resulting space charge density is reported in figure 2a.

The definition of a compact model needs a continuous function that provides the correct transition between the weak and strong inversion regions. The channel charge within the DG-MOSFET is determined by integrating the differential gate capacitance per unit of area, C_{gd}. The latter is given by $2C_gC_s/(2C_g + C_s)$, where C_s is the semiconductor capacitance and $2C_g$ is the gate capacitance. The definition of $2C_g$ already accounts for the extended space distribution of the channel charge within the semiconductor film, which never allows C_{gd} to reach, even asymptotically, the oxide capacitance $2C_{ox}$ (fig. 2b). The integration of C_{gd} gives

$$-Q_c = 2C_g \frac{k_BT}{q} \log\{1 + \exp\left[q(V_{GS} - V_T - V)/k_BT\right]\} , \tag{2}$$

where V_T is defined as the V_{GS} value at which the semiconductor capacitance equals the gate capacitance. This corresponds to the intersections of the curves in figure 2b with the horizontal line drawn at $C_{gd} = C_g$. Equation (2) provides a correct result both in weak and strong inversion.

Shockley's gradual channel approximation is assumed to hold. Under such condition, the drain current in strong inversion is expressed as usual and gives a similar equation to the standard form of the MOSFET characteristic:

$$I_D = 2\frac{W}{L}\frac{\mu_{no}C_g}{1 + \alpha_n V_{DS}}\left[(V_{GS} - V_T)V_{DS} - \frac{1}{2}V_{DS}^2\right] , \tag{3}$$

where $\alpha_n = \mu_{no}/(v_{sat}L)$. Two main features make it different: first, the DG-MOSFET is a three-terminal device, hence, the threshold voltage is not influenced by the body effect. Next, the quadratic form of its characteristic is rigorous, because the depletion charge is strictly constant in the DG-MOSFET channel. In subthreshold conditions,

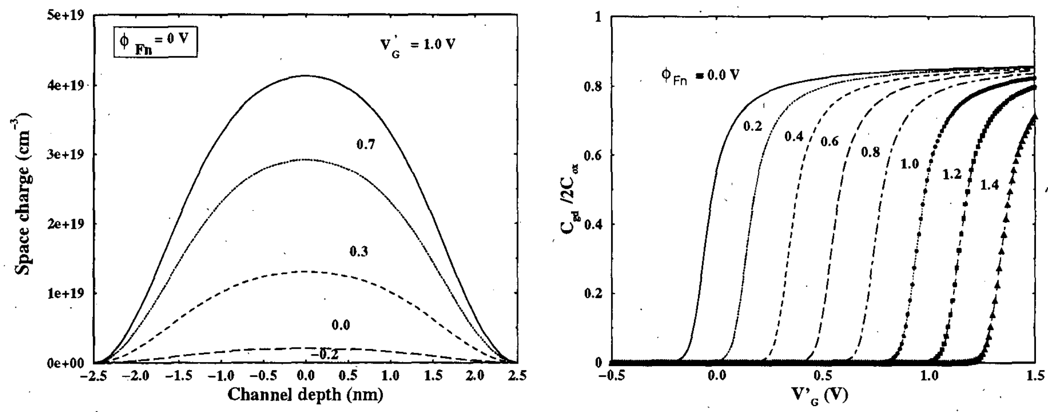

a b

Figure 2: a) Electron charge distribution within the silicon layer for different bias points. b) Normalized differential gate capacitance vs. gate voltage for different values of the quasi-Fermi potential. The curves show that C_{gd} never reaches the oxide capacitance.

the current expression exhibits an ideality factor equal to 1, thus, the slope of the DG-MOSFET current is about 60 mV/decade at room temperature. Moreover, the transit time of the carriers turns out to be about 0.2 psec.

Due to the extremely-short channel of the investigated device, the carrier behavior within the channel is expected to be quasi-ballistic, thus allowing a strong velocity overshoot to be reached. In order to estimate the influence of velocity overshoot on the device performance, we start with a simplified energy-balance model for a 2D electron gas. The non-local effect related with the gradual heating of the carriers along the channel is accounted for by a modified mobility expression, given by

$$\mu_n = \frac{\mu_{no}}{1 + \gamma_n V_{DS}}, \qquad \gamma_n = \frac{\mu_{n0}}{v_{sat} L} \frac{1}{(1 + 2\lambda_w/L)}, \tag{4}$$

which allows the carrier velocity to exceed the saturation velocity if the channel length becomes comparable with the energy-relaxation length λ_w.

3. Results

A wide set of Monte Carlo data have been collected by running a number of simulations using DAMOCLES [4]. More specifically, the I-V characteristics of an n-channel DG-MOSFET with 30 nm gate length, 5 nm semiconductor depth and 3 nm gate-oxide thickness were computed at different bias points. In order to compare the model calculations with Monte Carlo data, a transverse-field dependent mobility has been incorporated: as the normal field at the interface is proportional to the channel charge, the low-field mobility has been modeled as

$$\mu_{no} = \mu_o \left\{ 1 + \theta \frac{k_B T}{q} \log \left\{ 1 + \exp\left[q(V_{GS} - V_T)/k_B T \right] \right\} \right\}^{-1}, \tag{5}$$

where θ is a parameter that can be estimated with a fitting procedure on the I-V characteristics. In the saturation regime, the drain-induced barrier lowering is accounted for in order to reproduce the moderate rise of the current with V_{DS} in saturation. More specifically, a linear variation of the threshold voltage with V_{DS} is accounted for by simply substituting V_T with (V_T - ηV_{DS}). In the following figures, a factor $\eta = 80\,\mathrm{mV/V}$ has been assumed. The output characteristics of the DG-MOSFET are compared with self-consistent Monte Carlo simulations in figure 3a, showing a very reasonable agreement. By introducing the inversion-layer charge model, the drain current model can be used to correctly evaluate the transition between weak and strong inversion, as shown in figure 3b.

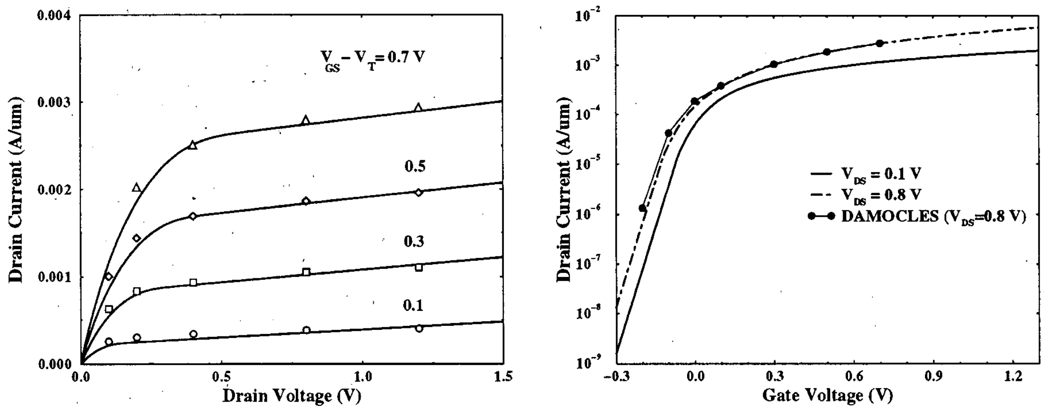

a b

Figure 3: Comparison of the DG-MOSFET characteristics. Solid lines: analytical model; symbols: Monte Carlo simulations. $\mu_{no} = 220\ \mathrm{cm}^2/\mathrm{Vsec}$, $v_{sat} = 8\times10^6\ \mathrm{cm/sec}$, $\theta = 0.2\ \mathrm{V}^{-1}$, $\eta = 80mV/V$. a) Output characteristics. b) Log-plot of drain current vs. $(V_{GS} - V_T)$.

4. Conclusions

In this work we have developed a compact model of the DG- MOSFET which accounts for charge quantization, Fermi statistics and non-static effects within the channel region. Rather surprisingly, the device equations can be reduced to a formalism which is similar to the standard MOSFET models, although some important differences affect, even substantially, the device behavior. The model provides a continuous transition of the MOSFET current between weak and strong inversion, and accounts for non-static effects which occur within the channel due to the comparable values of the channel and the energy-relaxation lengths.

References

[1] D. J. Frank, S. E. Laux, M. V. Fischetti *Proc. of the 1992 International Electron Device Meeting (IEDM)*, S. Francisco, Calif. p. 553-556, December 1992.

[2] F. Balestra, S. Cristoloveanu, M. Benachir, J. Brini, T. Elewa *IEEE Electron Device Letters*, vol. EDL-8, no. 9, pp. 410-412, September 1987.

[3] C. Fiegna, A. Abramo *Proc. of the 1997 International Electron Device Meeting (IEDM)*, S. Francisco, Calif., pp. 93-96, December 1997.

[4] S. Laux, M.V. Fischetti and D. Frank *IBM J. Res. Devel.*, vol. 34, p. 466, 1990.